Molecular Vision 2006; 12:1372-9 <http://www.molvis.org/molvis/v12/a154/>
Received 27 September 2006 | Accepted 6 November 2006 | Published 15 November 2006

The cataract-causing mutation G98R in human αA-crystallin leads to folding defects and loss of chaperone activity

Devendra Singh, Bakthisaran Raman, Tangirala Ramakrishna, Ch. Mohan Rao

Centre for Cellular and Molecular Biology, Hyderabad, India

Purpose: The objective of this study is to understand the molecular basis of cataract that develops due to the mutation of the glycine-98 residue to arginine in αA-crystallin.
Methods: The glycine-98 residue was mutated to arginine by site-directed mutagenesis. The expression, structural and chaperone properties and thermal stability of the mutant, G98RαA-crystallin have been studied. The secondary and tertiary structure of the wild type and the mutant protein was studied using circular dichroism and fluorescence spectroscopy. The quaternary structure was studied by gel filtration chromatography and dynamic light scattering. Chaperone activity studies were carried out using DTT-induced aggregation of insulin.
Results: Unlike the wild type protein, the heterologous expression of G98R αA-crystallin in *E.coli* results in the formation of inclusion bodies. Upon dissolving the inclusion bodies in 3 M urea and subjecting to refolding, it yielded a clear solution. The refolded mutant protein exhibits altered secondary, tertiary and quaternary structure, which lacks chaperone function, and is susceptible to heat-induced aggregation.
Conclusions: The G98R mutation in αA-crystallin results in altered folding and becomes aggregation-prone leading to formation of large oligomers lacking chaperone function. Tendency to aggregate and loss of chaperone activity could be contributing to turbidity and loss of transparency of the lens.

Molecular chaperones are a class of proteins that interact with partially unfolded states of other proteins and prevent off pathway processes, which lead to aggregation and inactivation, thus keeping them in a folding competent state. α-Crystallin is a major protein of the mammalian eye lens. It is a large multimeric protein comprised of two gene products, αA- and αB-crystallin, [1] which are present in molar ratio of 3:1 in the mammalian lens [2]. Both αA- and αB-crystallin have a subunit molecular mass of about 20 kDa. αA- and αB-crystallin share sequence homology with other members of the small heat shock protein family [3] and exhibit molecular chaperone-like activity in preventing the aggregation of other proteins [4-8], in protecting enzyme activity upon heat stress [9-12] and in helping some enzymes to refold [13-15].

α-Crystallin from old human lenses [16] and from selenite-induced cataractous lenses of an animal model [17] exhibit decreased chaperone-like activity. It is possible that α-crystallin chaperones the formation and maintenance of a transparent and refractive eye lens and may help maintain transparency by interacting with aged/damaged proteins. Point mutations in αA- as well as αB-crystallin have been reported to cause pathological conditions. The mutation of a highly conserved arginine residue (R116C in αA-crystallin) leads to congenital cataract [18], whereas in αB-crystallin (R120G) it leads to desmin-related myopathy as well as congenital cataract [19]. Studies from our laboratory [7] as well as those from other laboratories [20-22] have shown that mutation of this arginine residue causes altered secondary, tertiary and quaternary structure of αA- and αB-crystallin, which results in loss of chaperone-like activity. Subsequently, a few other mutations in αA- or αB-crystallin that lead to cataract have also been reported (Table 1). A recent study by Santhiya et al. [27] has reported the identification of a mutation in αA-crystallin (G98R) in three members of an Indian family that leads to onset of cataract at the age of 16 years. The molecular basis for the cataract caused by this mutation is not known. In the present study, we investigated the effect of this mutation on the structure and chaperone function of αA-crystallin. Our study shows that this mutation leads to folding defect and results in partially folded, aggregation-prone heterogeneous populations of very large oligomers, which lack chaperone activity.

Correspondence to: Dr. Ch. Mohan Rao, Ph.D., Deputy Director, Centre for Cellular and Molecular Biology, Uppal Road, Hyderabad 500 007, India; Phone: +91 40 27192543; FAX: +91 40 27160591; email: mohan@ccmb.res.in

METHODS

Materials: pET-21a(+) vector, T7 promoter and terminator primers were obtained from Novagen (Madison, WI). Gel filtration chromatographic medium Bio-Gel A-1.5m was purchased from Bio-Rad laboratories (Hercules, CA). Q-Sepharose, Superose-6 HR 10/30 and a high molecular weight protein calibration kit comprising of thyroglobulin, ferritin, catalase, and aldolase were purchased from Amersham Biosciences (Uppsala, Sweden). Insulin and dithiothreitol (DTT) were from Sigma (St. Louis, MO). 1,1'-bi(4-anilino)naphthalenesulfonic acid (Bis-ANS) was purchased from Molecular Probes (Eugene, OR).

Creating mutant of αA-crystallin: Recombinant human αA-crystallin gene cloned in pET-21a(+) was used as tem-

plate to generate mutant using polymerase chain reaction (PCR). Two independent PCRs were performed using T7 promoter primer and the mutagenic primer 5'-GTT GTG CTT TCT GTG GAT CTC CAC-3' as one primer pair and 5'-GTG GAG ATC CAC AGA AAG CAC AAC-3' and T7 terminator primer as the second primer pair. The resulting partially overlapping fragments were reamplified using T7 promoter and T7 terminator primers. The amplified fragment was digested and then ligated in the *Xba*I and *Hin*dIII sites of the pET-21a(+) expression vector. The sequence of this construct was verified by T7 promoter and terminator primers using 3700 ABI automated DNA sequencer.

Expression and purification of the recombinant wild type and G98R mutant protein: The wild type and the mutant recombinant proteins were over expressed in *Escherichia coli* BL21 (DE3) cells. Briefly, both bacterial cell pellets were suspended in 50 mM Tris-HCl, pH 7.2, containing 100 mM NaCl and 1 mM EDTA (TNE) buffer, sonicated, and centrifuged. The wild type protein which partitioned in the soluble fraction was purified essentially as described earlier [7]. The mutant protein partitioned into inclusion bodies, which were washed and dissolved in 50 mM Tris-HCl buffer, pH 7.2 containing 1 mM EDTA and 3 M urea. The solubilized inclusion bodies with mutant protein was directly subjected to ion exchange chromatography using a Q-Sepharose column equilibrated with the same buffer. The column was washed with 50 mM Tris-HCl buffer, pH 7.2 containing 1 mM EDTA and 150 mM NaCl without urea so that the protein was allowed to refold. The mutant protein was eluted with a step gradient of buffer containing 250 mM salt. The purified proteins were dialyzed against the TNE buffer and concentrated by ultra filtration. The purity of the wild type and mutant proteins was checked by sodium dodecylsulfate (SDS)-polyacrylamide gel electrophoresis and the proteins were found to be homogeneous. In an another experiment, the purified wild type αA-crystallin was similarly treated with 3 M urea and refolding to study the refolded protein. The concentrations of both the wild type and the mutant protein samples were estimated using its absorption coefficient at 280 nm as 0.725 at 1 mg/ml determined by a method described by Pace et al. [30].

Chaperone Assay: The chaperone-like activity of the wild type and mutant proteins was studied using insulin as the target protein as described earlier [31]. Insulin (0.2 mg/ml) in 10 mM phosphate buffer, pH 7.4, containing 150 mM NaCl was incubated in the absence or the presence of proteins at 37 °C. Aggregation was initiated by the addition of dithiothreitol (DTT) to a final concentration of 20 mM. The extent of aggregation was measured as a function of time by monitoring the

Table 1.

αA-crystallin		
Mutation	**Disease**	**Remarks**
R116C	Congenital zonular central nuclear opacity or cortical and posterior	Change in secondary, tertiary, quaternery structure and decreased chaperone-like activity [7, 20].
	Fan-shaped microcornea-cataract syndrome [24].	Increase in substrate binding and loss of chaperone-like activity [23].
R49C	Autosomal dominant nuclear cataract [25]	Abnormal localization to nucleus, failure to protect staurosporine-induced apoptosis [25].
		Recombinant protein, however, does not show significant changes in the secondary, tertiary, quaternery structure and chaperone-like activity (unpublished results).
W9X	Autosomal recessive cataract [26]	Aberrantly truncated - only results in 8 amino acids peptide.
G98R	Peripheral ring-like opacity to total cataract with advancing age [27]	Present study shows that Heterologous expression leads to aggregation and insolubilization. Refolded protein shows altered secondary, tertiary, quaternary struture and loss of chaperone activity.
αB-crystallin		
Mutation	**Disease**	**Remarks**
R120G	Desmin-related myopathy and congenital cataract [19]	Change in secondary, tertiary and quaternary structure and decreased chaperone-like activity [7,21,22].
450DelA	Autosomal dominant congenital posterior polar cataract [28]	Deletion causing a frameshift in codon 150 giving rise to aberrant protein of 184 residue [28]. The aberrant protein is not yet characterized.
D140N	Autosomal dominant congenital lamellar cataract [29]	Alterations in tertiary, quaternary structure and loss of chaperone-like activity [29].

Point mutations in α-crystallins that are associated with pathological conditions in human.

scattering at 465 nm in a Hitachi F-4000 fluorescence spectrophotometer.

Fluorescence studies: All fluorescence measurements were done using a Hitachi F-4500 fluorescence spectrophotometer. Intrinsic tryptophan fluorescence spectra of the wild type and the mutant α-crystallin (0.2 mg/ml) in TNE buffer were recorded by exciting the sample at 295 nm with excitation and emission band passes set at 2.5 nm each.

Binding of hydrophobic probe bis-ANS was studied by incubating 0.2 mg/ml of proteins samples with 10 μM of bis-ANS at 25 °C for 30 min. Fluorescence spectra were recorded from 400 to 600 nm with the excitation wavelength at 390 nm. The excitation and emission band passes were set at 2.5 nm each. All spectra were recorded in corrected spectrum mode.

Circular dichroism studies: Near and far UV circular dichroism (CD) spectra of the wild type and the mutant α-crystallin were recorded using a JASCO J-715 spectropolarimeter at 25 °C. All spectra reported are the average of 4 accumulations. Spectra were recorded using 1.0 mg/ml of protein in TNE buffer in a 1 cm path length cell for near UV region and using 0.5 mg/ml of protein in 0.1 cm path length cell for far UV region.

FPLC Gel Permeation Chromatography: Oligomeric sizes of the wild type and mutant proteins were evaluated on a Superose-6 HR 10/30 prepacked FPLC column (dimensions 1x30 cm). High molecular mass standards comprising thyroglobulin (669 kDa), ferritin (440 kDa), catalase (232 kDa) and aldolase (158 kDa) were used for calibration.

Dynamic light scattering studies: The hydrodynamic radii of the wild type and the mutant α-crystallin was measured using a Photocor Dynamic Light Scattering Instrument from Photocor Instruments Inc. (MD) at a 90° angle with a 633 nm 25 mW laser. The protein samples (3 mg/ml) were filtered through a 0.22 μ membrane and measurements made at 25 °C. The data were analyzed using Dynals version 2.0 software provided with the instrument.

Thermal aggregation of wild type and G98R mutant protein: Thermal aggregation of each protein was studied by recording the scattering at 465 nm in Flurolog-3 fluorescence spectrophotometer (Jobin Yvon, Edison, NJ) from 25 °C to 80 °C with an increment of 1 °C. Wild type and mutant proteins (0.2 mg/ml) in 10 mM phosphate buffer pH 7.4 containing 100 mM NaCl were incubated at each temperature for 2 min.

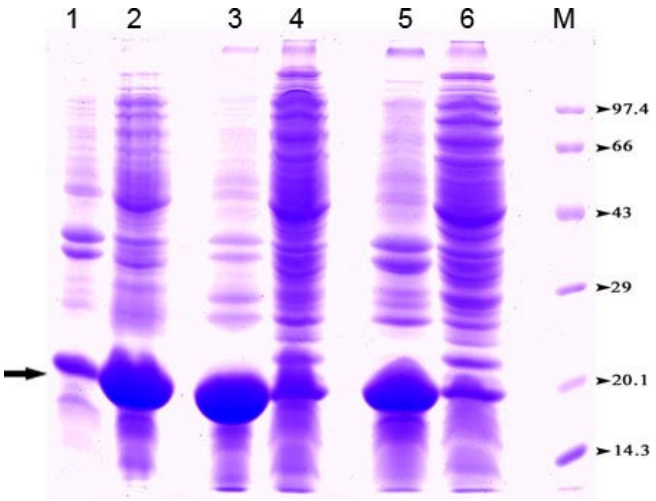

Figure 1. SDS-PAGE of soluble and insoluble fractions of *E.coli* BL21 (DE3) cells over expressing wild type and mutant αA crystallin at 37 °C and 30 °C. Lanes 1 and 2 represent the insoluble and soluble fractions, respectively of cells grown at 37 °C expressing the wild type αA crystallin indicating that most of the protein is present in the soluble fraction. Lanes 3 and 4 represent the insoluble and soluble fractions, respectively of cells grown at 37 °C expressing the mutant G98RαA crystallin, indicating that most of the mutant protein is present in the insoluble fraction. Lanes 5 and 6 represent the insoluble and soluble fractions, respectively of cells grown at 30 °C expressing the mutant G98R αA crystallin indicating that even at low temperature, the mutant protein goes in to the insoluble fraction. Lane M shows the positions of molecular mass markers. Arrow indicates the position of the wild type or the mutant αA crystallin.

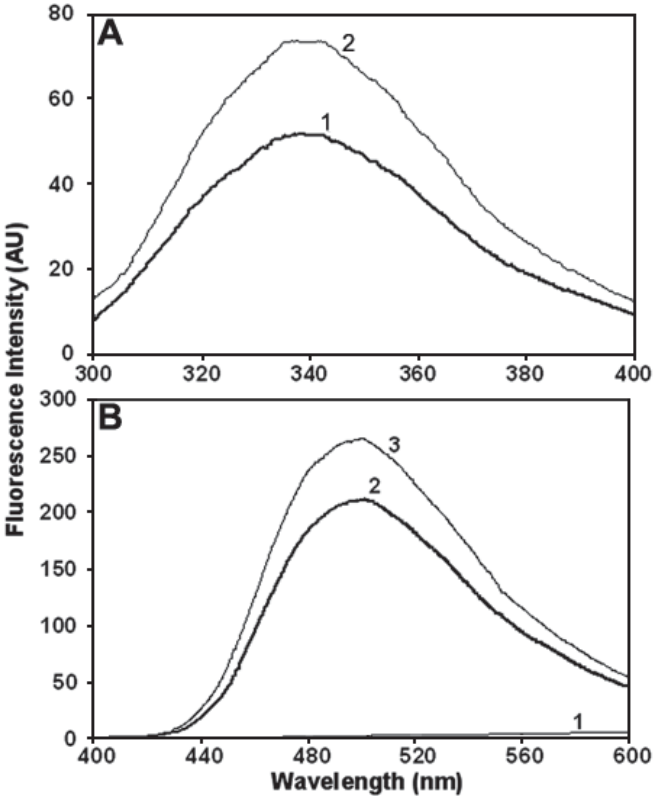

Figure 2. Intrinsic tryptophan fluorescence and bis-ANS binding of the wild type and G98R αA-crystallin. **A**: Intrinsic tryptophan fluorescence spectra of the wild type (curve 1) and the mutant (curve 2) αA-crystallin indicating that the mutant protein exhibits enhanced fluorescence intensity. A sample of 0.2 mg/ml the wild type or the mutant αA-crystallin in TNE buffer was used. The samples were excited at 295 nm. The excitation and emission band passes were set at 2.5 nm. **B**: Fluorescence spectra of bis-ANS (10 mM) in buffer alone (curve 1) and in the presence of 0.2 mg/ml wild type (curve 2) or G98R αA-crystallin (curve 3) indicating that the mutant protein exhibits relatively more bis-ANS binding. Excitation wavelength was set at 390 nm. The excitation and emission band passes were set at 2.5 nm.

RESULTS

To study the effect of G98R mutation in human αA-crystallin on the structure and chaperone activity of the protein, we have expressed the recombinant proteins in *E.coli* BL21 (DE3). Interestingly, contrary to the wild type αA-crystallin, the mutant protein almost exclusively partition in to insoluble fractions (Figure 1) when expressed in the bacterial cells, suggesting that the mutant protein forms inclusion bodies. We have also tested whether lowering the temperature during expression to 30 °C have any influence on the result as lowering the culture temperature results in better yield of soluble proteins in some cases of heterologous expression in bacterial cells [32,33]. However, even lowering temperature did not result in appreciable change in the solubility of the expressed mutant protein (Figure 1). We have also found that even after lowering the inducer (IPTG) concentration to one fifth or one tenth, the mutant protein remained in the insoluble fraction (data not shown). These results suggest that the mutant protein is aggregation prone in the cell which can not be rescued either by lowering temperature or the inducer concentration.

We dissolved the insoluble mutant protein in 3 M urea and subjected the protein to refolding (see the experimental procedure for details). The refolded protein remained in solution over prolonged periods of time. We, therefore, compared the structural and chaperone properties of the refolded mutant protein (referred as mutant protein or G98RαA-crystallin henceforth) with the wild type protein. Our earlier study showed that lens α-crystallin refolds completely from its denatured state in 8 M urea [34]. We also found that when the wild type αA-crystallin was treated with 3 M urea and sub-

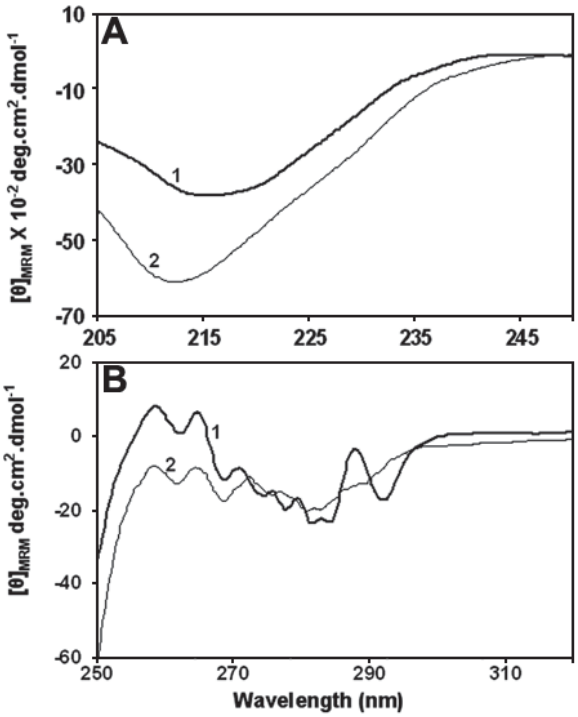

Figure 4. Circular dichroism (CD) spectra of wild type and G98R αA-crystallin. **A**: Far-UV CD spectra of the wild type (curve 1) and the mutant (curve 2) αA-crystallin indicating a significant change in the secondary structure of G98R αA-crystallin upon mutation. **B**: Near-UV CD spectra of the wild type (curve 1) and the mutant αA-crystallin (curve 2) indicating a loosening of the tertiary structural packing of G98R αA-crystallin upon mutation. $[\theta]_{MRM}$, mean residue mass ellipticity.

αA-crystallin

Amino acid sequence	IFLDVKHFSPEDLTVKVQDDFVEIHGKHNERQDDHGYISREFHRRYRLPSN
Chou-Fasman	EEEEEEE-----EEEEE---EEEE-----------EEEEEE-EEEE----
Garnier	EEEEE--------EEEE---EEEE-------------HHHHHHHH-----
Hydro moment	EEEEEEE-----EEEEE---EEEEE-----------HHHHHHHHHH----
GOR4	EEE----------EE-----HHHHH----------HHHHHH--------
SSpro8	EEEEEE--GTG-EEEEE--EEEEH--------TTSEE-HHHHHHE------
nnPredict	EEEE---------EE-----HHHHH----------H-HHHH--------
Jpred	EEEE--------EEEEE---EEEEEEEE--------EEEEEEEEEE----

G98R αA-crystallin

Amino acid sequence	IFLDVKHFSPEDLTVKVQDDFVEIHRKHNERQDDHGYISREFHRRYRLPSN
Chou-Fasman	EEEEEEE-----EEEEE---HHHHHHH---------EEEEEE-EEEE----
Garnier	EEEEE--------EEEE---HHHHHHH--HHH------HHHHHHHH-----
Hydro moment	EEEEEEE-----EEEEE---HHHHHH----------HHHHHHHHHH----
GOR4	EEE----------EE----HHHHHHHH---------HHHHHH--------
SSpro8	EEEEEE--GTG-EEEE-HHHHHHHHHH-H---TTTHE-HHHHHHE------
nnPredict	EEEE---------EE-----HHHHH----------H-HHHH--------
Jpred	EEEE--------EEEEE---EEEEEEEE--------EEEEEEEEEE----

Figure 3. Prediction of the secondary structural propensity of the sequence of the wild type and G98R αA-crystallin by various programs using different algorithms. The full-length sequences were subjected to predictions using Chou-Fasman, Garnier, hydrophobic moment (using software PepTool Lite 1.1), GOR4, SSpro8, nnPredict, Jpred programmes. Secondary structural propensities of the sequence from residue 73 to 123 are shown. Some of the programs predict a change in propensity from strand (E) in the wild type to helical (H) in the mutant in the sequence surrounding the mutated amino acid (shown in red). H, helix; E, extended strand; T, turn; G, 3_{10} helix; S, bend and Dashed line, random coil.

jected to refolding, it refolded to its native state regaining its structural and chaperone properties (data not shown).

Figure 2A shows the intrinsic tryptophan fluorescence spectra of the wild type and the mutant proteins. The emission maximum (338 nm) is not significantly altered upon mutation. However, fluorescence spectrum of the mutant protein exhibits significantly higher fluorescence intensity than that of the wild type protein. This shows that the microenvironment around the sole tryptophan residue of αA-crystallin is slightly perturbed in the mutant. We have probed the accessible hydrophobic surfaces of the wild type and the mutant protein using the hydrophobic fluorescent probes bis-ANS [35,36]. Figure 2B shows the fluorescence spectra of bis-ANS bound to the wild type and the mutant αA-crystallin. The fluorescence intensity of the probe in the presence of the mutant protein is found to be higher compared to that of the probe in the presence of the wild type protein suggesting an increase in the accessible hydrophobic surface of the protein upon mutation. Studies using ANS as a probe also yielded similar results.

We have analyzed the secondary structure propensities of the region around the G98 residue in αA-crystallin and the changes upon mutating the G to R by some secondary structural prediction programs. Some of these algorithms predict a conversion of beta sheet propensities to alpha helix upon G to R change in the sequence (Figure 3). Far UV CD study indicates a change in the secondary structure (Figure 4A). The spectrum of the mutant protein shows significant differences compared to that of the wild type protein: the wild type αA-crystallin exhibit a minimum around 216 nm which is shifted towards lower wavelength (212) for the mutant protein. The mutant protein also exhibits increased ellipticity. It is possible that the region of the sequence bearing the mutation which has strand propensity in the wild type is significantly perturbed in the mutant protein. Increase in ellipticity and apparent shift of minimum to 210 nm from 216 nm indicate possible increase in helical content. Figure 4B compares the near UV-CD spectra of the wild type and mutant αA-crystallin. It is evident from the figure that the side chain packing of the aromatic residues are significantly affected in the mutant protein. The fine structure seen in the region between 270 to 300 nm of the near UV-CD spectrum of αA-crystallin is lost in the spectrum of the mutant with overall decreased ellipticity. This result indicates that G98R mutation leads to tertiary structural alterations leading to decreased chirality at the aromatic residues.

We have investigated the quaternary structure of the wild type and the mutant proteins by dynamic light scattering and gel-filtration chromatography. The dynamic light scattering study shows the hydrodynamic radius of the wild type αA-crystallin to be 9.14 nm (with standard error of 0.07 for 7 experiments). The hydrodynamic radius of the mutant protein was determined to be 15.13 nm (with standard error of 0.19 for 7 experiments) indicating that a large oligomeric status of the mutant protein. Consistent with the dynamic light scattering study, gel filtration chromatography shows that the mutant protein elute prior to the wild type protein indicating the size of the mutant protein is significantly large compared to that of the wild type αA-crystallin (Figure 5). Estimation of the molecular mass of these proteins using the elution volumes of the standard proteins showed 680 kDa and 1020 kDa for the wild type and the mutant protein, respectively.

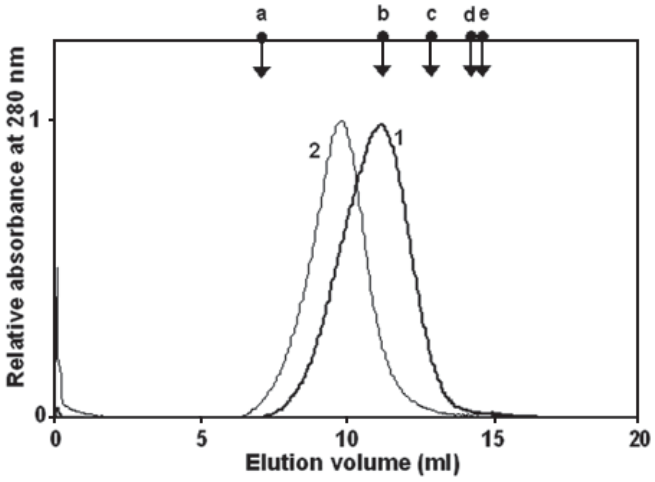

Figure 5. Gel-filtration chromatography of wild type and G98R αA-crystallin on a Superpose 6 HR10/30 FPLC column. Elution profiles of the wild type (curve 1) and the mutant (curve 2) αA-crystallin show that the mutant forms relatively larger oligomeric assembly. The elution positions of molecular mass standards are indicated by down arrows. a, blue dextran (2000 kDa); b, thyroglobulin (669 kDa); c, ferritin (440 kDa); d, catalase (232 kDa); e, aldolase (158 kDa).

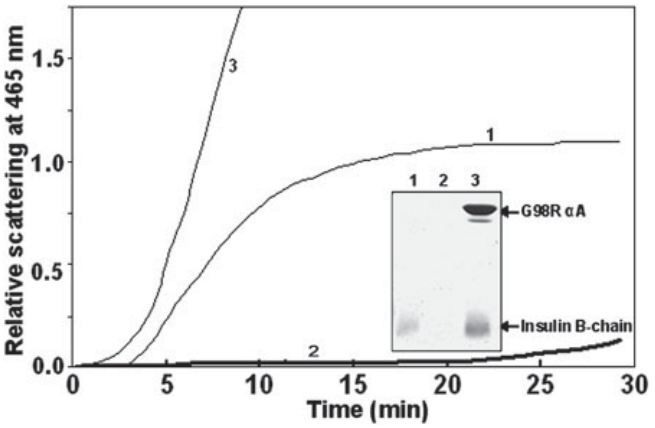

Figure 6. G98R mutation in αA-crystallin leads to loss of chaperone-like activity towards DTT-induced aggregation of insulin. Aggregation of insulin (0.2 mg/ml), as monitored by light scattering at 465 nm, was initiated by the addition of 20 mM DTT in the absence (curve 1) or in the presence of 0.2 mg/ml wild type (curve 2) or the mutant (curve 3) αA-crystallin. Inset shows that the mutant protein co-aggregates with the insulin B-chain as analyzed by SDS-PAGE. The pellet obtained after centrifuging (at 10000x g for 20 min) the samples (after DTT-induced aggregation for 30 min) was subjected to electrophoresis on a 17% SDS-Polyacrylamide gel: Samples are insulin alone (lane 1), insulin in the presence of the wild type (lane 2), or the mutant (lane 3) αA-crystallin.

Thus, all our results show that the mutant protein exhibit altered secondary and tertiary structures and assembles in to large oligomers. Figure 6 compares the chaperone-like activity of the wild type and the mutant αA-crystallin towards DTT-induced aggregation of insulin. The wild type protein at 1:1 (w/w) ratio prevents the aggregation of insulin almost completely. On the other hand, the mutant protein at the same ratio did not prevent the aggregation of insulin. Rather the scattering increases dramatically in the presence of the mutant protein. Thus, the result indicates that the mutation results in complete loss of chaperone activity of αA-crystallin.

Earlier studies have shown that hydrophobic interactions are involved in the chaperone-like activity of α-crystallin [5,37]. Sharma et al. [38-40] have identified target protein binding sites and bis-ANS binding sites in both αA- and αB-crystallin and found some overlapping sites (consisting of hydrophobic residues). It is surprising that even though the mutant protein exhibit slightly more bis-ANS binding compared to the wild type protein (Figure 2B), it exhibits no chaperone activity. The loss of activity could be ascribed to two possible reasons: (1) loss or decreased target protein binding ability, or (2) decreased solubility of the target protein and chaperone complex. Since the mutant protein binds bis-ANS, it is likely that the target protein binding ability of the mutant protein is not affected. Moreover, the light scattering of the insulin-G98R complex is significantly higher (even in comparison to aggregated insulin alone) suggesting an interaction between the mutant and target protein. We have, therefore, analyzed the aggregates formed in the presence of mutant protein by SDS-PAGE. The B-chain of insulin aggregates and precipitates out while the A-chain remains soluble upon reducing the disulfide bonds of insulin with DTT [41]. As shown in the Figure 6 the wild type αA-crystallin prevents the aggregation of insulin almost completely. When this sample was centrifuged and a pellet, if any, was subjected to SDS-PAGE, no bands corresponding to insulin B-chain or αA-crystallin could be seen (lane 2 in the inset to Figure 6). A similar experiment with the mutant protein results in very high scattering. SDS-PAGE of the pellet obtained after centrifuging this sample, showed distinct bands corresponding to insulin B-chain as well as the mutant αA-crystallin (lane 3 in the inset to Figure 6) indicating that both insulin B-chain and the mutant proteins co-aggregate. Insulin aggregates formed at an early stage might act as seed for aggregation-prone mutant αA-crystallin leading to coaggregation and precipitation. In order to test this possibility, we have added aggregates of insulin B-chain prepared separately (in buffer alone) to a sample of the mutant protein and monitored the light scattering for 1 h and did not find increase in the light scattering. This result rules out the possibility of nucleation of aggregation of the mutant αA-crystallin by the aggregating insulin B-chain. Therefore, it is likely that the complex of the mutant and the insulin B-chain is aggregation-prone or insoluble.

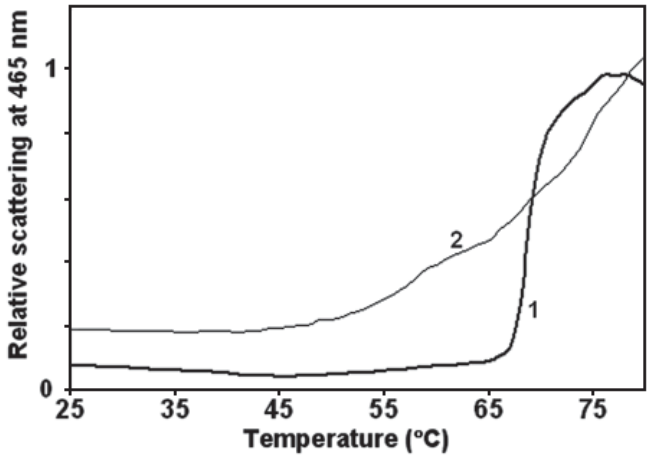

Figure 7. G98R mutation in αA-crystallin leads to decreased thermal stability. Aggregation of the wild type (curve 1) or the mutant (curve 2) αA-crystallin was monitored by light scattering at 465 nm as a function of temperature.

α-Crystallins are generally stable as they do not exhibit unfolding to a great extents even at elevated temperatures [8,42,43]. However, they undergo subtle structural perturbations. Earlier circular dichroism, infrared spectroscopy and calorimetric studies on calf-eye lens α-crystallin and recombinant human αA- or αB-crystallin have reported a transition between 55 °C to 65 °C indicating structural alterations [8,42-45]. When we monitored light scattering of the wild type αA-crystallin, we observed a sharp increase in light scattering at elevated temperature. We, therefore, compared the thermal stability in terms of its self-aggregation of the wild type and the mutant αA-crystallin (Figure 7). The light scattering of the sample of the wild type protein remains unchanged up to 65 °C, beyond which there is a sharp increase indicating aggregation of the protein; possibly by a cooperative process judging by the sharp transition. The mutant protein as such exhibits high light scattering compared to the wild type protein due to its large oligomeric size. Contrary to the cooperative behavior of the wild type protein, the mutant protein show gradual increase in the light scattering above 45 °C and is more pronounced beyond 60 °C. These results show altered structural stability and increased tendency for aggregation.

DISCUSSION

A putative cataract causing mutation of G98R in αA-crystallin has been recently identified in an Indian family [27]. The molecular basis of this mutation, however, is not known. Our present study provides some insight in to the molecular basis for the pathology. Unlike the earlier reported missense mutants of αA- or αB-crystallin (Table 1), almost all the expressed G98R αA-crystallin goes into the inclusion bodies in *E.coli* suggesting that the mutation leads to folding defects that result in aggregation in cells. The refolded mutant protein shows altered secondary, tertiary, and quaternary structure and lacks chaperone activity compared to wild type αA-crystallin. It is to be noted that the mutation (G98R) is in one of the beta-strands of the core "α-crystallin domain". Thus the mutation can disrupt or significantly alter the "immunoglobulin" fold [46,47] of the domain due to the introduction of charge, bulkiness of the R residue and its high helical propensity. Such

alteration in the secondary structure can lead to overall changes in the tertiary and quaternary structure.

Our study also shows that though the mutant protein has the ability to interact with the target protein, the complex is aggregation-prone or insoluble, providing the molecular mechanism for the loss of its chaperone function. A recent study shows that R116C αA-crystallin, which exhibits decreased chaperone activity [7,20], in fact binds strongly to the target protein [23]. Our present study taken together with that of Koteiche and Mchaourab [23] indicates that these mutations result in conformational alterations that affect the solubility of or impart aggregation propensity to the complex rather than decreasing their target protein-binding ability.

As mentioned earlier, the mutant G98RαA-crystallin forms inclusion bodies when it is expressed in *E.coli*. It is possible that in the crowded in vivo environment of the cell, the mutant protein exhibits folding defects and forms aggregates. The propensity for aggregation of the mutant is also reflected in its thermo-stability (Figure 7). It is possible that the lack of chaperone-like activity and tendency to aggregate may cause lens turbidity and cataract in the case of G98R mutation. Such a molecular defect leading to improper folding would be expected to cause congenital cataract. However, the cataract formation ascribed to G98R mutation is not congenital; its onset occurs at the age of 16 years [27]. The reason for the time lag is not clear at the moment. It is possible that other chaperone molecules such as αB-crystallin or wild type αA-crystallin of the hetero allele (heterozygous) might keep the mutant protein from aggregating and delay the onset of cataract. It is also possible that other damaged or aged proteins bind to the mutant form and the aggregation-prone complex tends to accumulate with time leading to eventual compromise of transparency, causing presenile cataract. Our study, inter alia, demonstrates that the mutant G98RαA-crystallin aggregates when complexed with the target protein.

We conclude that the G98R mutation results in altered secondary and tertiary structures, decreased thermo-stability and large oligomer formation. These changes in the structure lead to loss of chaperone property. The folding defects of the mutant and its tendency to aggregate either alone or upon binding to target protein may contribute to cataract formation in the affected individuals.

ACKNOWLEDGEMENTS

We thank Abhay Kumar Thakur for his help in fluorescence experiments. D.S. acknowledges the CSIR, New Delhi for the grant of Senior Research Fellowship.

REFERENCES

1. Quax-Jeuken Y, Quax W, van Rens G, Khan PM, Bloemendal H. Complete structure of the alpha B-crystallin gene: conservation of the exon-intron distribution in the two nonlinked alpha-crystallin genes. Proc Natl Acad Sci U S A 1985; 82:5819-23.
2. Sax CM, Piatigorsky J. Expression of the alpha-crystallin/small heat-shock protein/molecular chaperone genes in the lens and other tissues. Adv Enzymol Relat Areas Mol Biol 1994; 69:155-201.
3. Ingolia TD, Craig EA. Four small Drosophila heat shock proteins are related to each other and to mammalian alpha-crystallin. Proc Natl Acad Sci U S A 1982; 79:2360-4.
4. Horwitz J. Alpha-crystallin can function as a molecular chaperone. Proc Natl Acad Sci U S A 1992; 89:10449-53.
5. Raman B, Rao CM. Chaperone-like activity and quaternary structure of alpha-crystallin. J Biol Chem 1994; 269:27264-8.
6. Sun TX, Das BK, Liang JJ. Conformational and functional differences between recombinant human lens alphaA- and alphaB-crystallin. J Biol Chem 1997; 272:6220-5.
7. Kumar LV, Ramakrishna T, Rao CM. Structural and functional consequences of the mutation of a conserved arginine residue in alphaA and alphaB crystallins. J Biol Chem 1999; 274:24137-41.
8. Datta SA, Rao CM. Differential temperature-dependent chaperone-like activity of alphaA- and alphaB-crystallin homoaggregates. J Biol Chem 1999; 274:34773-8.
9. Rajaraman K, Raman B, Ramakrishna T, Rao CM. Interaction of human recombinant alphaA- and alphaB-crystallins with early and late unfolding intermediates of citrate synthase on its thermal denaturation. FEBS Lett 2001; 497:118-23.
10. Hook DW, Harding JJ. Molecular chaperones protect catalase against thermal stress. Eur J Biochem 1997; 247:380-5.
11. Marini I, Moschini R, Del Corso A, Mura U. Complete protection by alpha-crystallin of lens sorbitol dehydrogenase undergoing thermal stress. J Biol Chem 2000; 275:32559-65.
12. Hess JF, FitzGerald PG. Protection of a restriction enzyme from heat inactivation by [alpha]-crystallin. Mol Vis 1998; 4:29.
13. Goenka S, Raman B, Ramakrishna T, Rao CM. Unfolding and refolding of a quinone oxidoreductase: alpha-crystallin, a molecular chaperone, assists its reactivation. Biochem J 2001; 359:547-56.
14. Rawat U, Rao M. Interactions of chaperone alpha-crystallin with the molten globule state of xylose reductase. Implications for reconstitution of the active enzyme. J Biol Chem 1998; 273:9415-23.
15. Nath D, Rawat U, Anish R, Rao M. Alpha-crystallin and ATP facilitate the in vitro renaturation of xylanase: enhancement of refolding by metal ions. Protein Sci 2002; 11:2727-34.
16. Cherian M, Abraham EC. Decreased molecular chaperone property of alpha-crystallins due to posttranslational modifications. Biochem Biophys Res Commun 1995; 208:675-9.
17. Kelley MJ, David LL, Iwasaki N, Wright J, Shearer TR. alpha-Crystallin chaperone activity is reduced by calpain II in vitro and in selenite cataract. J Biol Chem 1993; 268:18844-9.
18. Litt M, Kramer P, LaMorticella DM, Murphey W, Lovrien EW, Weleber RG. Autosomal dominant congenital cataract associated with a missense mutation in the human alpha crystallin gene CRYAA. Hum Mol Genet 1998; 7:471-4.
19. Vicart P, Caron A, Guicheney P, Li Z, Prevost MC, Faure A, Chateau D, Chapon F, Tome F, Dupret JM, Paulin D, Fardeau M. A missense mutation in the alphaB-crystallin chaperone gene causes a desmin-related myopathy. Nat Genet 1998; 20:92-5.
20. Shroff NP, Cherian-Shaw M, Bera S, Abraham EC. Mutation of R116C results in highly oligomerized alpha A-crystallin with modified structure and defective chaperone-like function. Biochemistry 2000; 39:1420-6.
21. Bova MP, Yaron O, Huang Q, Ding L, Haley DA, Stewart PL, Horwitz J. Mutation R120G in alphaB-crystallin, which is linked to a desmin-related myopathy, results in an irregular structure and defective chaperone-like function. Proc Natl Acad Sci U S A 1999; 96:6137-42.

22. Perng MD, Muchowski PJ, van Den IJssel P, Wu GJ, Hutcheson AM, Clark JI, Quinlan RA. The cardiomyopathy and lens cataract mutation in alphaB-crystallin alters its protein structure, chaperone activity, and interaction with intermediate filaments in vitro. J Biol Chem 1999; 274:33235-43.
23. Koteiche HA, Mchaourab HS. Mechanism of a hereditary cataract phenotype. Mutations in alphaA-crystallin activate substrate binding. J Biol Chem 2006; 281:14273-9.
24. Vanita V, Singh JR, Hejtmancik JF, Nuernberg P, Hennies HC, Singh D, Sperling K. A novel fan-shaped cataract-microcornea syndrome caused by a mutation of CRYAA in an Indian family. Mol Vis 2006; 12:518-22.
25. Mackay DS, Andley UP, Shiels A. Cell death triggered by a novel mutation in the alphaA-crystallin gene underlies autosomal dominant cataract linked to chromosome 21q. Eur J Hum Genet 2003; 11:784-93.
26. Pras E, Frydman M, Levy-Nissenbaum E, Bakhan T, Raz J, Assia EI, Goldman B, Pras E. A nonsense mutation (W9X) in CRYAA causes autosomal recessive cataract in an inbred Jewish Persian family. Invest Ophthalmol Vis Sci 2000; 41:3511-5.
27. Santhiya ST, Soker T, Klopp N, Illig T, Prakash MV, Selvaraj B, Gopinath PM, Graw J. Identification of a novel, putative cataract-causing allele in CRYAA (G98R) in an Indian family. Mol Vis 2006; 12:768-73.
28. Berry V, Francis P, Reddy MA, Collyer D, Vithana E, MacKay I, Dawson G, Carey AH, Moore A, Bhattacharya SS, Quinlan RA. Alpha-B crystallin gene (CRYAB) mutation causes dominant congenital posterior polar cataract in humans. Am J Hum Genet 2001; 69:1141-5.
29. Liu Y, Zhang X, Luo L, Wu M, Zeng R, Cheng G, Hu B, Liu B, Liang JJ, Shang F. A novel alphaB-crystallin mutation associated with autosomal dominant congenital lamellar cataract. Invest Ophthalmol Vis Sci 2006; 47:1069-75.
30. Pace CN, Vajdos F, Fee L, Grimsley G, Gray T. How to measure and predict the molar absorption coefficient of a protein. Protein Sci 1995; 4:2411-23.
31. Raman B, Ramakrishna T, Rao CM. Temperature dependent chaperone-like activity of alpha-crystallin. FEBS Lett 1995; 365:133-6.
32. Schein CH. Production of soluble recombinant proteins in bacteria. Bio/Technology 1989; 7:1141-1149.
33. Sorensen HP, Mortensen KK. Soluble expression of recombinant proteins in the cytoplasm of Escherichia coli. Microb Cell Fact 2005; 4:1.
34. Raman B, Ramakrishna T, Rao CM. Rapid refolding studies on the chaperone-like alpha-crystallin. Effect of alpha-crystallin on refolding of beta- and gamma-crystallins. J Biol Chem 1995; 270:19888-92.
35. Musci G, Metz GD, Tsunematsu H, Berliner LJ. 4,4'-Bis[8-(phenylamino)naphthalene-1-sulfonate] binding to human thrombins: a sensitive exo site fluorescent affinity probe. Biochemistry 1985; 24:2034-9.
36. Shi L, Palleros DR, Fink AL. Protein conformational changes induced by 1,1'-bis(4-anilino-5-naphthalenesulfonic acid): preferential binding to the molten globule of DnaK. Biochemistry 1994; 33:7536-46.
37. Das KP, Surewicz WK. Temperature-induced exposure of hydrophobic surfaces and its effect on the chaperone activity of alpha-crystallin. FEBS Lett 1995; 369:321-5.
38. Sharma KK, Kaur H, Kester K. Functional elements in molecular chaperone alpha-crystallin: identification of binding sites in alpha B-crystallin. Biochem Biophys Res Commun 1997; 239:217-22.
39. Sharma KK, Kumar GS, Murphy AS, Kester K. Identification of 1,1'-bi(4-anilino)naphthalene-5,5'-disulfonic acid binding sequences in alpha-crystallin. J Biol Chem 1998; 273:15474-8.
40. Sharma KK, Kumar RS, Kumar GS, Quinn PT. Synthesis and characterization of a peptide identified as a functional element in alphaA-crystallin. J Biol Chem 2000; 275:3767-71.
41. Sanger F. Fractionation of oxidized insulin. Biochem J 1949; 44:126-8.
42. Raman B, Rao CM. Chaperone-like activity and temperature-induced structural changes of alpha-crystallin. J Biol Chem 1997; 272:23559-64.
43. Reddy GB, Das KP, Petrash JM, Surewicz WK. Temperature-dependent chaperone activity and structural properties of human alphaA- and alphaB-crystallins. J Biol Chem 2000; 275:4565-70.
44. Surewicz WK, Olesen PR. On the thermal stability of alpha-crystallin: a new insight from infrared spectroscopy. Biochemistry 1995; 34:9655-60.
45. Walsh MT, Sen AC, Chakrabarti B. Micellar subunit assembly in a three-layer model of oligomeric alpha-crystallin. J Biol Chem 1991; 266:20079-84.
46. Mornon JP, Halaby D, Malfois M, Durand P, Callebaut I, Tardieu A. alpha-Crystallin C-terminal domain: on the track of an Ig fold. Int J Biol Macromol 1998; 22:219-27.
47. van Montfort RL, Basha E, Friedrich KL, Slingsby C, Vierling E. Crystal structure and assembly of a eukaryotic small heat shock protein. Nat Struct Biol 2001; 8:1025-30.

The print version of this article was created on 15 Nov 2006. This reflects all typographical corrections and errata to the article through that date. Details of any changes may be found in the online version of the article.